9-27-2019

Inhibition of Integrin $\alpha_d\beta_2$-Mediated Macrophage Adhesion to End Product of Docosahexaenoic Acid (DHA) Oxidation Prevents Macrophage Accumulation During Inflammation

Kui Cui
Quillen-Dishner College of Medicine

Nataly P. Podolnikova
Arizona State University

William Bailey
Quillen-Dishner College of Medicine, baileywp@etsu.edu

Eric Szmuc
Quillen-Dishner College of Medicine

Eugene A. Podrez
Cleveland Clinic Foundation

See next page for additional authors

Citation Information

Cui, Kui; Podolnikova, Nataly P.; Bailey, William; Szmuc, Eric; Podrez, Eugene A.; Byzova, Tatiana V.; and Yakubenko, Valentin P.. 2019. Inhibition of Integrin $\alpha_d\beta_2$-Mediated Macrophage Adhesion to End Product of Docosahexaenoic Acid (DHA) Oxidation Prevents Macrophage Accumulation During Inflammation. *Journal of Biological Chemistry*. Vol.294(39). 14370-14382. https://doi.org/10.1074/jbc.RA119.009590
PMID: 31395659 ISSN: 0021-9258

Inhibition of Integrin $\alpha_d\beta_2$-Mediated Macrophage Adhesion to End Product of Docosahexaenoic Acid (DHA) Oxidation Prevents Macrophage Accumulation During Inflammation

Creator(s)

Kui Cui, Nataly P. Podolnikova, William Bailey, Eric Szmuc, Eugene A. Podrez, Tatiana V. Byzova, and Valentin P. Yakubenko

Inhibition of integrin $\alpha_D\beta_2$–mediated macrophage adhesion to end product of docosahexaenoic acid (DHA) oxidation prevents macrophage accumulation during inflammation

Received for publication, May 30, 2019, and in revised form, July 22, 2019 Published, Papers in Press, August 8, 2019, DOI 10.1074/jbc.RA119.009590

Kui Cui[‡], Nataly P. Podolnikova[§], William Bailey[‡], Eric Szmuc[‡], Eugene A. Podrez[¶], Tatiana V. Byzova[¶], and Valentin P. Yakubenko[‡1]

From the [‡]Department of Biomedical Sciences, Quillen College of Medicine, East Tennessee State University, Johnson City, Tennessee 37614, [§]Center for Metabolic and Vascular Biology, School of Life Sciences, Arizona State University, Tempe, Arizona 85281, and [¶]Lerner Research Institute, Cleveland Clinic, Cleveland, Ohio 44106

Edited by Dennis R. Voelker

A critical step in the development of chronic inflammatory diseases is the accumulation of proinflammatory macrophages in the extracellular matrix (ECM) of peripheral tissues. The adhesion receptor integrin $\alpha_D\beta_2$ promotes the development of atherosclerosis and diabetes by supporting macrophage retention in inflamed tissue. We recently found that the end product of docosahexaenoic acid (DHA) oxidation, 2-(ω-carboxyethyl)-pyrrole (CEP), serves as a ligand for $\alpha_D\beta_2$. CEP adduct with ECM is generated during inflammation-mediated lipid peroxidation. The goal of this project was to identify a specific inhibitor for $\alpha_D\beta_2$–CEP interaction that can prevent macrophage accumulation. Using a specially designed peptide library, Biacore-detected protein–protein interaction, and adhesion of integrin-transfected HEK 293 cells, we identified a sequence (called P5 peptide) that significantly and specifically inhibited α_D–CEP binding. In the model of thioglycollate-induced peritoneal inflammation, the injection of cyclic P5 peptide reduced 3-fold the macrophage accumulation in WT mice but had no effect in α_D-deficient mice. The tracking of adoptively transferred, fluorescently labeled WT and $\alpha_D^{-/-}$ monocytes in the model of peritoneal inflammation and *in vitro* two-dimensional and three-dimensional migration assays demonstrated that P5 peptide does not affect monocyte transendothelial migration or macrophage efflux from the peritoneal cavity but regulates macrophage migration through the ECM. Moreover, the injection of P5 peptide into WT mice on a high-fat diet prevents macrophage accumulation in adipose tissue in an $\alpha_D\beta_2$-dependent manner. Taken together, these results demonstrate the importance of $\alpha_D\beta_2$-mediated macrophage adhesion for the accumulation of infiltrating macrophages in the inflamed ECM and propose P5 peptide as a potential inhibitor of atherogenesis and diabetes.

Chronic inflammation is an essential mechanism during the development of cardiovascular and metabolic diseases. Monocyte recruitment and subsequent macrophage accumulation in the damaged tissue are critical steps that regulate inflammatory response and disease progression (1, 2). Although monocyte recruitment during acute inflammatory response may have a protective effect, the excessive accumulation of macrophages at the site of inflammation can lead to strong proinflammatory signaling, damage to healthy tissue, and development of chronic inflammation (3). Leukocyte integrins are adhesive receptors that significantly contribute to the monocyte/macrophage migration and accumulation (4). Integrin $\alpha_D\beta_2$ (CD11d/CD18) is the most recently discovered leukocyte integrin (5) with a unique expression pattern and specific role in inflammation. Recently, we and others demonstrated that $\alpha_D\beta_2$ has a relatively low expression on neutrophils and monocytes in circulation (6, 7) but is up-regulated on tissue macrophages, particularly in atherosclerotic lesions and adipose tissue during diabetes (8–10) (Table S1). We revealed that high expression of $\alpha_D\beta_2$ on the cell surface promotes a strong adhesion to ECM[2] proteins that leads to the retention of proinflammatory macrophages in inflamed tissue and supports atherogenesis and insulin resistance (11, 12).

Interestingly, $\alpha_D\beta_2$ shares a high level of homology and ligand binding properties with related integrin $\alpha_M\beta_2$ (CD11b/CD18; Mac-1) (13). $\alpha_M\beta_2$ is a well-studied leukocyte receptor, which is involved in the regulation of many acute and chronic inflammatory diseases (14–17). $\alpha_D\beta_2$ and $\alpha_M\beta_2$ shares many extracellular matrix ligands such as fibronectin, fibrinogen, and vitronectin; however, the expression of these integrins is markedly different on distinct subsets of macrophages (11). Particularly, $\alpha_D\beta_2$ has a low expression on resident and alternatively activated (M2) macrophages but is dramatically up-regulated on classically activated (M1) macrophages. $\alpha_M\beta_2$ demonstrates a high expression on resident macrophages but is expressed moderately on M1 and M2 macrophages. This difference determines the distinct role of $\alpha_D\beta_2$ and $\alpha_M\beta_2$ in macrophage

This work was supported by National Institutes of Health Grants DK102020 (to V. P. Y.), HL071625 (to T. V. B.), HL077213 (to E. A. P.), and C06RR0306551 (to East Tennessee State University). The authors declare that they have no conflicts of interest with the contents of this article. The content is solely the responsibility of the authors and does not necessarily represent the official views of the National Institutes of Health.
This article contains Figs. S1–S3 and Table S1.

[1] To whom correspondence should be addressed: Dept. of Biomedical Sciences, Quillen College of Medicine, East Tennessee State University, P. O. Box 70582, Johnson City, TN 37614. Tel.: 423-439-8511; E-mail: yakubenko@etsu.edu.

[2] The abbreviations used are: ECM, extracellular matrix; DHA, docosahexaenoic acid; CEP, 2-(ω-carboxyethyl)pyrrole; HUVEC, human umbilical vein endothelial cell; MCP-1, monocyte chemoattractant protein 1; MIDAS, metal ion–dependent adhesion site; HEK, human embryonic kidney; Fg, fibrinogen; IFNγ, interferon γ.

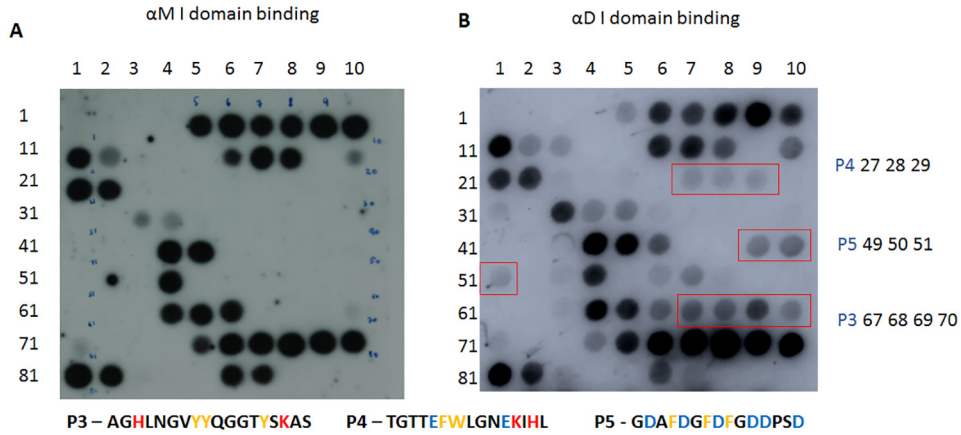

Figure 1. Screening the peptide library for binding to α_D and α_M I-domains. The peptide library was synthetized on the cellulose membrane spanning the sequence of the γ-module of fibrinogen. The library was incubated with ^{125}I-labeled α_D I-domain or α_M I-domain, and binding was visualized by autoradiography. The *numbers* on the *left* and *above* each panel indicate the peptide (spot) numbers. The peptide numbers correspond to the numbering of spots in the panel. Spot analysis indicated three peptides, called P3, P4, and P5, as unique sequences that bind to $\alpha_D\beta_2$ (shown in red boxes).

migration/retention and contribution to the development of inflammatory diseases (12). Particularly, recent data have demonstrated that $\alpha_M\beta_2$ has a protective effect on the development of atherosclerosis and diabetes (16, 18), which is opposite to the pathological role of $\alpha_D\beta_2$ in chronic inflammation.

Ligand recognition, followed by specific intracellular signaling, is a critical step that determines integrin-mediated leukocyte migration and cellular responses. Most recently, we found that the end product of DHA oxidation, 2-(ω-carboxyethyl)pyrrole (CEP), serves as a specific inflammatory ligand for integrins $\alpha_D\beta_2$ and $\alpha_M\beta_2$ (19). CEP is formed during the oxidation of DHA that leads to the formation of CEP adducts with ECM proteins (20, 21). These CEP-modified proteins support $\alpha_M\beta_2$- and $\alpha_D\beta_2$-mediated macrophage migration to the site of inflammation. CEP is formed mostly during inflammation and was abundantly detected in atherosclerotic lesions and adipose tissue during diabetes (22, 23). Based on the $\alpha_D\beta_2$-specific pattern of expression on M1 macrophages, we hypothesized that CEP can be a critical ligand for $\alpha_D\beta_2$-mediated macrophage retention at the site of inflammation, particularly because the affinity of α_D to CEP surpasses the affinity to natural ECM proteins (13, 19).

Therefore, the inhibition of $\alpha_D\beta_2$-mediated adhesion of macrophages to CEP-modified proteins in the ECM may have a strong anti-inflammatory effect. However, the overlapping ligand binding properties of $\alpha_M\beta_2$ and $\alpha_D\beta_2$ complicate the development of an effective inhibitor (13, 24).

In this project, we developed a strategy to identify the amino acid sequences that are specific only for integrin $\alpha_D\beta_2$ and have no effect on $\alpha_M\beta_2$. Using *in vitro* approaches, we selected the peptide, called P5, with strong blocking ability against $\alpha_D\beta_2$–CEP interaction. Applying the model of peritoneal inflammation, we demonstrated that P5 peptide significantly reduced the accumulation of macrophages in the peritoneal cavity, and this effect was directly related to the $\alpha_D\beta_2$-dependent migration via ECM. Moreover, P5 does not interfere with monocyte transmigration through endothelium or macrophage efflux from the peritoneal cavity. Finally, using the model of diet-induced diabetes, we demonstrated that P5 peptide markedly inhibits the accumulation of macrophages in the adipose tissue of mice, which demonstrates the effect of P5 on the development of chronic inflammation. Taken together, these data confirm the significant role of integrin $\alpha_D\beta_2$ during an inflammatory response, support the concept of $\alpha_D\beta_2$ as an important anti-inflammatory target, and propose the P5 sequence as a potential inhibitor of inflammation.

Results

Screening the peptide library for binding to α_D and α_M I-domains

To identify the sequences that are unique for $\alpha_D\beta_2$ binding and have no cross-reactivity with $\alpha_M\beta_2$ binding, we synthesized a peptide library on the cellulose membrane spanning the sequence of the γ-module of fibrinogen (Fig. S1). It has been shown that the γ-module of fibrinogen contains multiple binding sites for $\alpha_M\beta_2$ integrin (25) and is critical for $\alpha_D\beta_2$ binding to fibrinogen (13). The peptide library consisting of 9-mer peptides with a 3-residue offset was tested for binding of ^{125}I-labeled active α_D I-domain as described previously for α_M I-domain (25) (Fig. 1). We detected three sequences, which are specific only for the binding of α_D I-domain (spots 27–29, 49–51, and 67–70). The identified sequences, AGHLNGVYYQGGTYSKAS, TGTTEFWLGNEKIHL, and GDAFDGFDFGDDPSD, were synthesized as soluble peptides and named P3, P4, and P5, correspondingly.

Evaluation of inhibitory abilities of identified sequences by surface plasmon resonance and adhesion assay

The abilities of detected peptides to inhibit α_D I-domain binding to CEP were tested by applying surface plasmon resonance (Biacore 3000) (Fig. 2, *A* and *B*). α_D I-domain and α_M I-domain were preincubated with 200 μg/ml P3 (106.8 μM), P4 (114.6 μM), and P5 (126.8 μM) peptides and added to the immobilized CEP using previously detected concentrations (19). Two peptides (P4 and P5) demonstrated marked inhibition of α_D I-domain binding, whereas inhibition of α_M I-domain was not significant. To extend this result, we tested peptides in the adhesion assay using $\alpha_D\beta_2$- and $\alpha_M\beta_2$-transfected HEK 293 cells (Fig. 2*C*). CEP was immobilized on the 96-well plate, and integrin-transfected cell lines were preincubated with 200

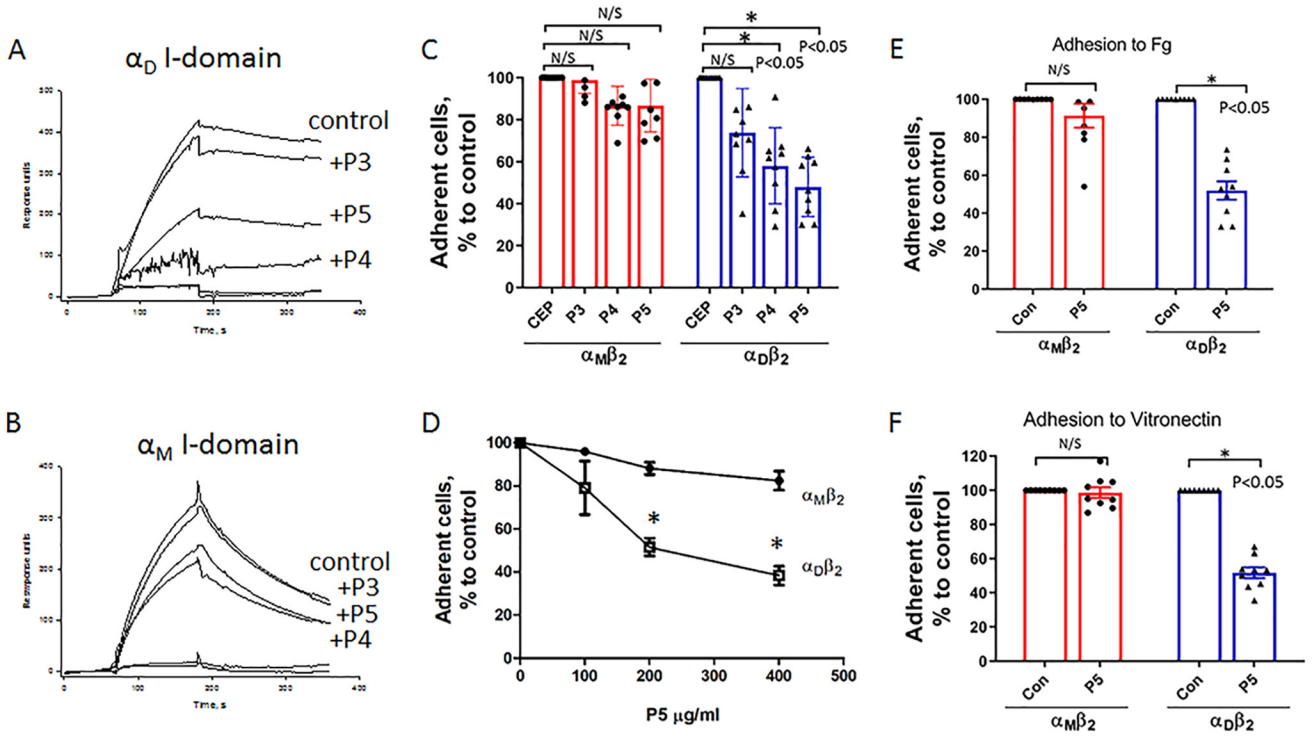

Figure 2. P5 peptide is a specific inhibitor for integrin $\alpha_D\beta_2$. *A* and *B*, representative profiles of the surface plasmon resonance measured by Biacore for α_D (*A*) and α_M (*B*) binding to CEP-BSA coupled to the CM5 chip in the presence of 200 μg/ml P3 (106.8 μM), P4 (114.6 μM), and P5 (126.8 μM) peptides. *C* and *D*, adhesion assay of $\alpha_D\beta_2$- and $\alpha_M\beta_2$-transfected HEK 293 cells in the presence of inhibitory peptides. *C*, a 96-well plate was coated with CEP for 3 h at 37 °C. Calcein AM–labeled HEK 293 cells transfected with $\alpha_M\beta_2$ and $\alpha_D\beta_2$ were added to the wells, and cell adhesion was determined after 30 min in a fluorescence plate reader. Some samples were preincubated with P3, P4, or P5 peptide for 20 min before the adhesion assay. Data are presented as mean ± S.E. *, $p < 0.05$. *D*, adhesion of HEK 293 cells transfected with $\alpha_M\beta_2$ and $\alpha_D\beta_2$ to CEP in the presence of different concentrations of P5 peptide. Data are presented as mean ± S.E. *, $p < 0.05$. *E* and *F*, adhesion of HEK 293 cells transfected with $\alpha_M\beta_2$ and $\alpha_D\beta_2$ to fibrinogen (*E*) and vitronectin (*F*). Some samples were preincubated with P5 peptide before the adhesion assay. Data are presented as mean ± S.E. (*error bars*). *, $p < 0.05$. *N/S*, not significant.

μg/ml peptides. Similar to direct protein–protein assay, P3 peptide did not have a blocking effect. However, the inhibitory ability of P4 peptide was reduced compared with direct protein–protein interaction assay (Fig. 2*A*). Apparently, the binding region for the P4 peptide is only exposed on isolated I-domain, but it is partially blocked on $\alpha_D\beta_2$ heterodimer, which is expressed on the cell surface. Therefore, P4-binding site is not a natural region for the $\alpha_D\beta_2$–CEP interaction. In contrast to these data, P5 peptide inhibited 50% of $\alpha_D\beta_2$ adhesion to CEP, which was similar to the Biacore results. The effect of P5 peptide on adhesion of $\alpha_M\beta_2$ cells was not significant. We tested different concentrations of P5 peptide in adhesion assays and found concentration-dependent inhibition of $\alpha_D\beta_2$ binding to CEP (Fig. 2*D*).

Integrins $\alpha_D\beta_2$ and $\alpha_M\beta_2$ are multiligand receptors (13, 24). It has been shown that several integrin ligands have overlapping binding sites within the I-domain (24, 27-29). Based on this information, we tested whether P5 peptide can inhibit $\alpha_D\beta_2$-mediated cell adhesion to other ligands. First, we evaluated the adhesion of $\alpha_D\beta_2$- and $\alpha_M\beta_2$-transfected HEK 293 cells to fibrinogen in the presence of P5 peptide. We found that P5 peptide blocked only the adhesion of $\alpha_D\beta_2$ (Fig. 2*E*) in a concentration-dependent manner (Fig. 2*A*). Because integrin $\alpha_X\beta_2$, which is also expressed on macrophages, has high homology with α_D and interacts with fibrinogen (Fg), we tested this receptor in an inhibition assay. The adhesion of $\alpha_X\beta_2$-transfected cells to immobilized fibrinogen was not affected in the presence of P5 peptide (Fig. S2*B*), which confirmed the specificity of selected inhibitor for integrin α_D.

We also tested the ability of P5 to block the adhesion of $\alpha_D\beta_2$ and $\alpha_M\beta_2$ to another ligand, vitronectin, and received a similar result. Namely, P5 inhibits the adhesion of $\alpha_D\beta_2$-transfected cells but has no effect on adhesion of $\alpha_M\beta_2$-transfected cells (Fig. 2*F*). Taken together, these data demonstrated that P5 peptide can prevent the binding of $\alpha_D\beta_2$ to different ECM ligands without affecting the function of other macrophage integrins.

P5 peptide supports direct adhesion of $\alpha_D\beta_2$ cells and prevents receptor activation on the cell surface

The blocking peptide can bind directly to the binding site within α_D or may have an allosteric effect. To detect the mechanism of P5 inhibition, we tested the direct binding of $\alpha_D\beta_2$ to P5 peptide. Using immobilized P5 in an adhesion assay (Fig. 3*A*), we found that P5 peptide can support direct binding to $\alpha_D\beta_2$, whereas $\alpha_M\beta_2$ does not have this ability. The adhesion of both cell lines to Fg was used as a positive control (Fig. 3*A*).

The role of α_D I-domain conformation for the binding to P5 peptide was assessed using biolayer interferometry. Particularly, we tested the interaction of α_D I-domain in active and nonactive conformations to the biotinylated P5 peptide, which was immobilized on a streptavidin biosensor. We found that active form of α_D I-domain has a similar binding to P5 in the presence of 1 mM Mg^{2+} and 5 mM EDTA. At the same time, a

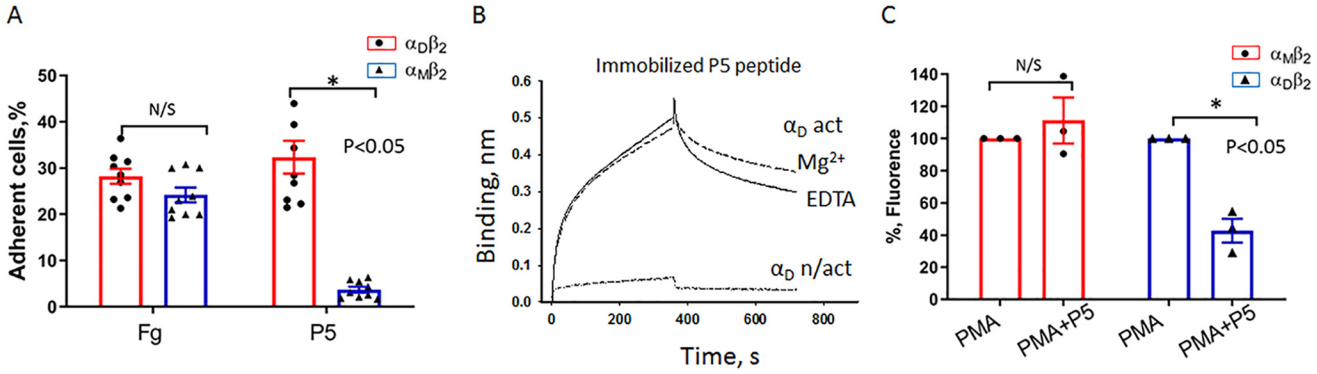

Figure 3. Characterization of P5 peptide binding to integrin $\alpha_D\beta_2$. *A*, direct adhesion of HEK 293 cells transfected with $\alpha_M\beta_2$ and $\alpha_D\beta_2$ to immobilized P5 peptide. Cells were added to a 96-well plate coated with P5 peptide or with Fg as control, and adhesion was performed as described in Fig. 2. *B*, analysis of the activation stage of α_D I-domain for binding to P5 peptide. A representative binding curve of α_D I-domain binding to P5 peptide was measured by biolayer interferometry (ForteBio). N-terminally biotinylated P5 peptide was immobilized on a streptavidin biosensor. 2 μM α_D I-domain in active (*solid line*) and nonactive conformations (*dotted line*) in the presence of 1 mM Mg^{2+} or α_D I-domain in active conformation in the presence of 5 mM EDTA (*dashed line*) was incubated with immobilized P5. The binding was analyzed using ForteBio Data Analysis 11.0 software. The experiment was repeated three times with similar results. *C*, P5 peptide inhibits the activation of integrin $\alpha_D\beta_2$ on the cell surface. $\alpha_D\beta_2$- and $\alpha_M\beta_2$-transfected HEK 293 cells were preincubated with P5 peptide for 30 min at 37 °C, and then cells were incubated with 100 nM phorbol 12-myristate 13-acetate (*PMA*) for 30 min at 37 °C to induce integrin activation. The activation stage of integrins was assessed using activation-dependent antibody mAb24. Fluorescently labeled cells were detected by FACS. Data are presented as mean ± S.E. (*error bars*). *, $p < 0.05$. *N/S*, not significant.

nonactive conformation of α_D I-domain could not interact with P5 (Fig. 3*B*).

In a parallel experiment, we tested how binding of P5 peptide affected the change in the conformation of the entire $\alpha_D\beta_2$ heterodimer on the cell surface. Using activation-dependent antibody mAb24, we found that preincubation with P5 peptide significantly reduced $\alpha_D\beta_2$ activation (Fig. 3*C*). Therefore, the binding of P5 peptide does not require a fully active conformation of $\alpha_D\beta_2$ and can prevent a conformational change from the intermediate to the active stage. In agreement with our other data, P5 peptide did not have an effect on the activation of $\alpha_M\beta_2$ cells.

Effect of P5 peptide on macrophage accumulation in the peritoneal cavities of WT, $\alpha_D^{-/-}$, and $\alpha_M^{-/-}$ mice

The blocking effect of P5 peptide on $\alpha_D\beta_2$-mediated cell adhesion might interfere with macrophage migration *in vivo*. We used the model of thioglycollate-induced peritoneal inflammation to evaluate changes in macrophage migration after P5 treatment. WT mice were injected intraperitoneally with P5 peptide or control peptide 30 min before the injection of thioglycollate, and the number of peritoneal macrophages was detected after 72 h. We selected a control peptide from the same γ-module sequence based on the absence of binding to $\alpha_D\beta_2$ and $\alpha_M\beta_2$ and presence of negatively and positively charged amino acids. Accordingly, the sequence (WNGRTSTADYAMFKV), which corresponds to spots 37–40, was synthetized and tested. The adhesion assay in the presence of the control peptide confirmed the lack of its effect on $\alpha_D\beta_2$-mediated adhesion (Fig. 4*A*). The injection of cyclic P5 peptide to WT mice reduced 3-fold the accumulation of macrophages in the peritoneal cavity, whereas the treatment with the control peptide or PBS had no effect (Fig. 4*B*). Interestingly, the injection of P5 to α_M-deficient mice demonstrated a reduction of macrophages in the peritoneal cavity similar to WT mice, whereas α_D deficiency completely eliminated the blocking effect of P5 peptide (Fig. 4*C*). These results demonstrate the specificity of P5 peptide *in vivo*.

Mechanism of P5 peptide inhibition during peritoneal inflammation

The model of peritoneal inflammation is a well-described model of acute inflammation that is commonly used to evaluate monocyte/macrophage recruitment. Macrophage accumulation in the peritoneal cavity depends on several factors, including monocyte progenitor translocation to the blood stream, monocyte transmigration via the endothelium monolayer, macrophage migration through the interstitium to the peritoneal cavity, and efflux from the cavity to the lymphatics. We sought to detect the step of macrophage accumulation with which P5 peptide interferes.

To clarify this question, we developed several assays. First, we isolated monocyte progenitors from WT mice, labeled cells with PKH26 red fluorescent dye, and injected them intravenously to the mice with initiated peritoneal inflammation (Fig. 5*A*). One group of mice was treated with P5 peptide; the second was treated with the control. After 72 h, cells were isolated from the peritoneal cavity, and the number of red fluorescent, adoptively transferred macrophages was evaluated by FACS (Fig. 5*B*). We found that according to our previous observations (Fig. 4*B*) the total number of macrophages was significantly reduced after P5 treatment (Fig. 5*C*, *left panel*). More interestingly, the number of labeled macrophages was also significantly decreased (Fig. 5*C*, *right panel*). This result demonstrated the effect of P5 peptide on macrophage recruitment, but clearly P5 does not affect translocation from bone marrow because labeled cells were injected to the blood stream. Also, this result shows that the effect of P5 is mediated by monocyte-derived macrophages and is not related to the proliferation of resident macrophages.

Second, we tested the potential role of P5 in macrophage efflux from the peritoneal cavity (Fig. 6*A*). Macrophages were isolated at 72 h after thioglycollate injection and labeled with PKH26 fluorescent dye. The labeled macrophages were injected intraperitoneally to the mice at 48 h after thioglycollate-induced inflammation. One group was treated immedi-

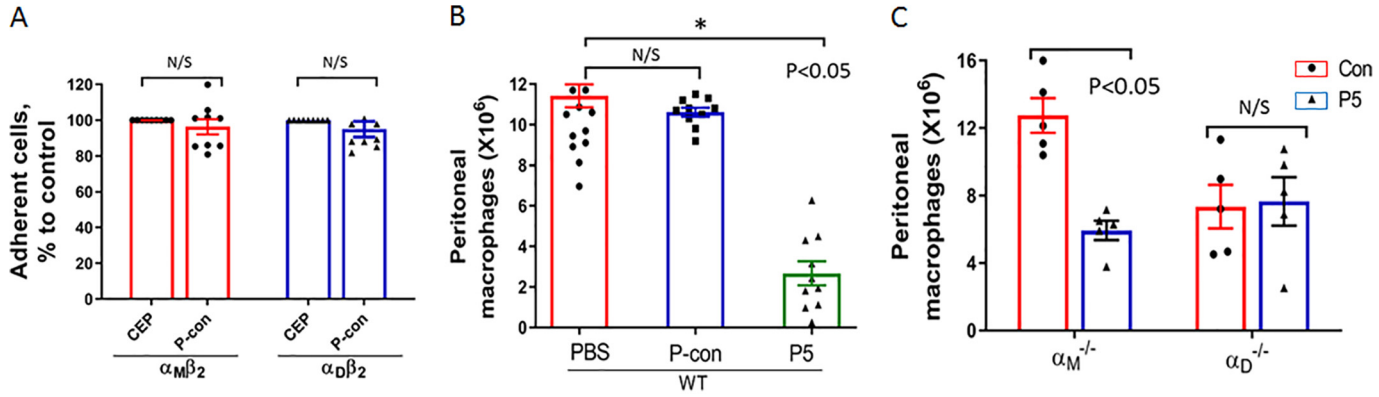

Figure 4. P5 peptide inhibits the accumulation of macrophages in the peritoneal cavity during sterile inflammation. *A*, adhesion of $\alpha_D\beta_2$- and $\alpha_M\beta_2$-transfected cells to CEP in the presence of 200 μg/ml control (57.2 μM) peptide (*P-con*). *B* and *C*, WT (*B*) and $\alpha_M^{-/-}$ and $\alpha_D^{-/-}$ (*C*) mice were intraperitoneally injected with 100 μg/mouse cyclic P5 (63.4 μM) peptide, control peptide, or PBS. 20 min later, 4% thioglycollate was injected intraperitoneally to all mice to induce inflammation. After 3 days, the amounts of WT, $\alpha_M^{-/-}$, and $\alpha_D^{-/-}$ macrophages were evaluated by assessing the number and percentage of macrophages in the inflamed peritoneal cavities of mice. Isolated peritoneal cells were counted, and the numbers of WT, $\alpha_M^{-/-}$, and $\alpha_D^{-/-}$ macrophages were calculated based on the percentage of F4/80-positive population in flow cytometry analysis. Data are presented as mean ± S.E. (*error bars*). *, $p < 0.05$. *N/S*, not significant.

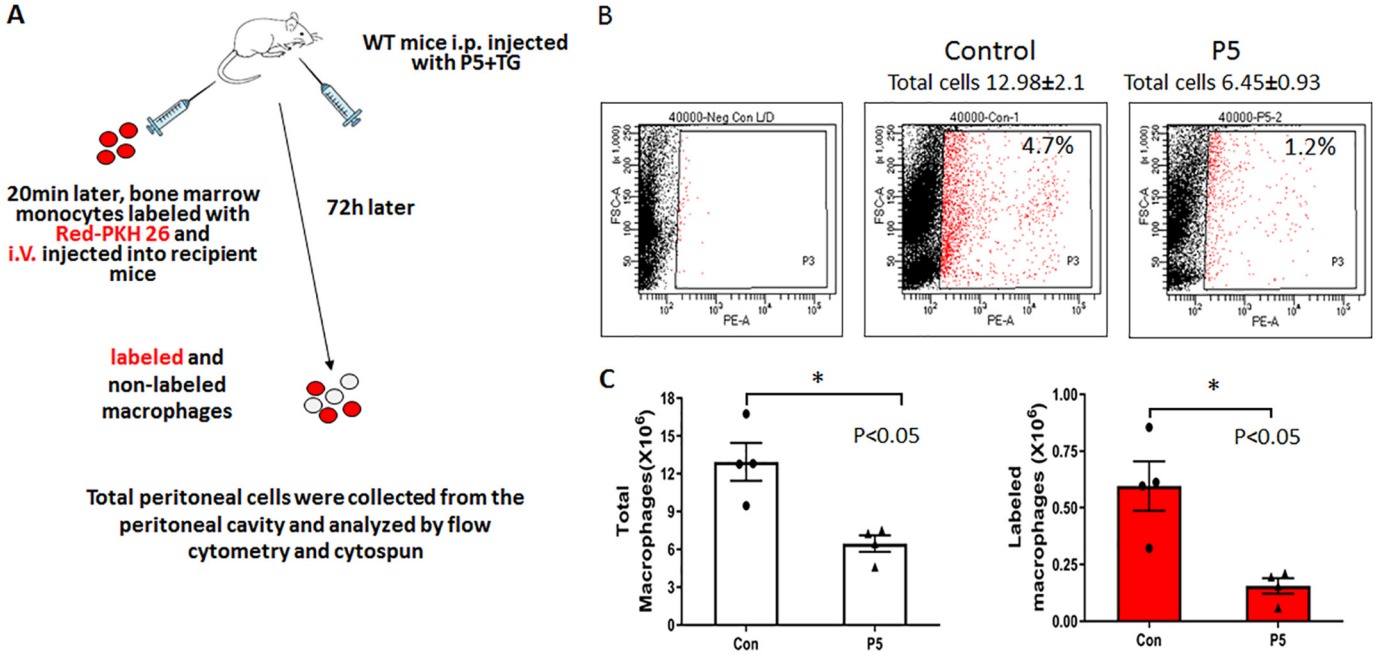

Figure 5. P5 peptide regulates the recruitment of macrophages. *A*, schematic representation of the experiment. Bone marrow–derived monocytes were isolated from donor WT mice and labeled with a red fluorescent dye, PKH26. Recipient WT mice were intraperitoneally injected with P5 peptide and 20 min later with 4% thioglycollate (*TG*) to induce inflammation. Then fluorescently labeled monocytes were injected into the tail veins of the recipient mice. After 72 h, the numbers of total macrophages and labeled macrophages were assessed by flow cytometry (*B*). The total macrophage number was calculated based on the percentage of F4/80-positive population in flow cytometry analysis. The labeled macrophage number was assessed based on the percentage of red-positive cells and the total number of macrophages in the sample (*C*). Data are presented as mean ± S.E. (*error bars*). *, $p < 0.05$. *Con*, control.

ately with P5 peptide; another group was treated with the control. After an additional 24 h, cells from the peritoneal cavity were collected, and the number of labeled macrophages was compared in both groups using FACS (Fig. 6*B*) and cytospin (Fig. S3). Again, the number of recipient macrophages was affected by P5 peptide (Fig. 6*C*). However, the amount of fluorescently labeled macrophages in the peritoneal cavity was not changed in the presence of P5 peptide, which demonstrates that P5 treatment did not affect efflux of macrophages during peritoneal inflammation (Fig. 6*C*).

Based on these experiments, we concluded that P5 interferes with the recruitment of monocytes/macrophages from the bloodstream to the peritoneal cavity. Therefore, the contribution of P5 peptide may affect endothelial transmigration or migration through the ECM.

P5 peptide has no effect on 2D transendothelial migration but inhibits 3D migration in the matrix

Accordingly, we tested the role of P5 in monocyte transmigration via endothelial monolayer *in vitro*. A Boyden chamber was coated overnight with human umbilical vein endothelial cells (HUVECs), which were labeled with green PKH67 fluorescent dye. Monocytes, labeled with red fluorescence (PKH26), were added to the upper chamber (Fig. 7*A*). Monocyte migra-

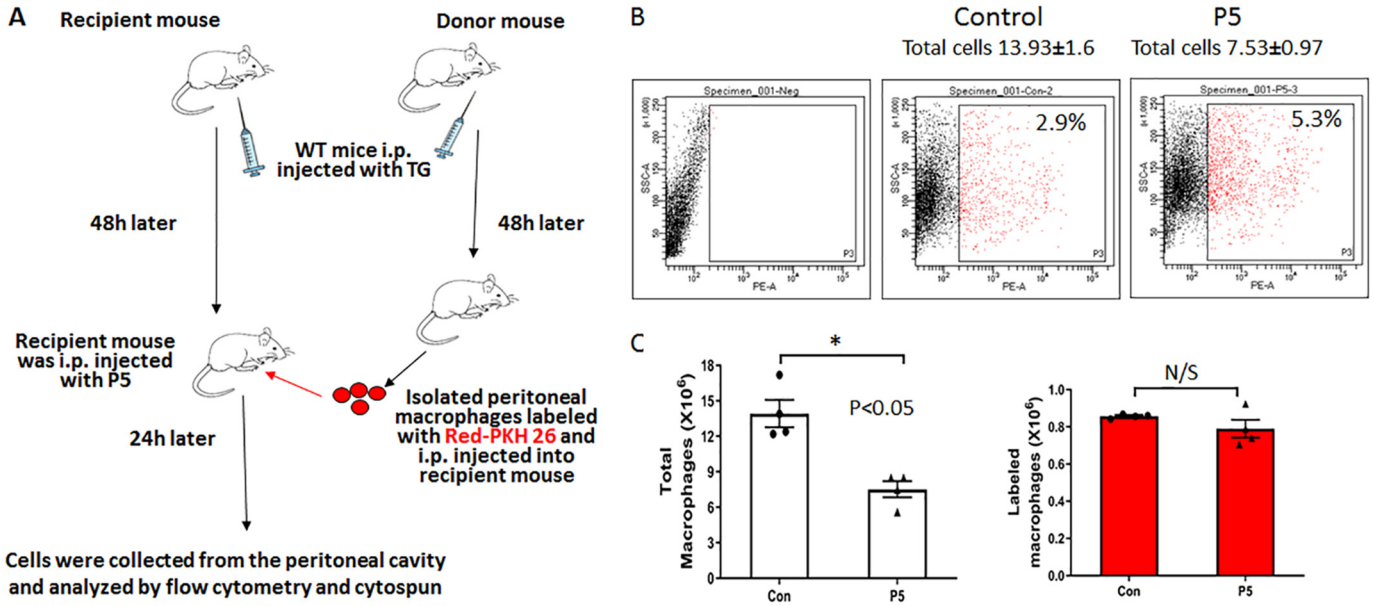

Figure 6. P5 peptide does not affect the efflux of macrophages from the peritoneal cavity. *A*, schematic representation of the experiment. Recipient and donor WT mice were intraperitoneally injected with thioglycollate (*TG*). After 48 h, macrophages were isolated from the peritoneal cavities of donor mice and labeled with a red fluorescent dye (PKH26). The recipient mice were intraperitoneally injected with labeled macrophages and P5 peptide. After an additional 24 h, the total macrophage number and percentage of labeled macrophages were evaluated by flow cytometry as described for Fig. 5. *B* and *C*, data are presented as mean ± S.E. (*error bars*). *, $p < 0.05$. *N/S*, not significant.

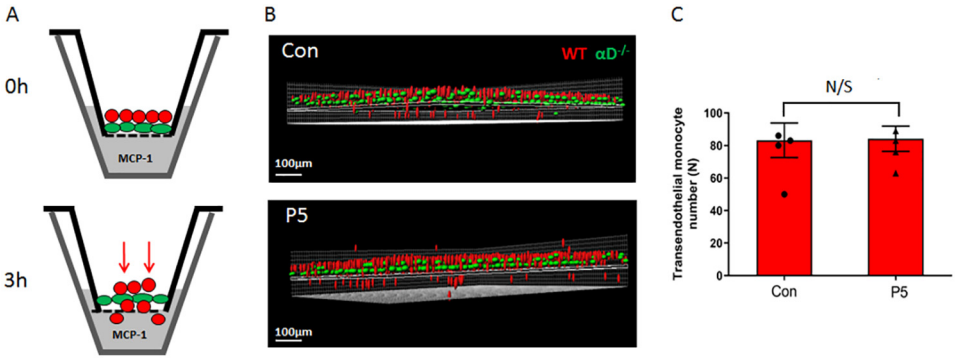

Figure 7. P5 peptide does not affect the transendothelial migration of monocytes. *A*, PKH67-fluorescently labeled (*green*) HUVECs were coated on the membrane of the upper chamber of the Transwell. Monocytes were labeled with PKH26 red fluorescent dye and added on top of endothelial cells. MCP-1 was added to the lower chamber of the Transwells to stimulate monocyte migration. After 3 h, monocyte transmigration was detected by a Leica confocal microscope. *B*, side view of the Transwell. In the P5 group, the monocytes were preincubated with P5 peptide for 20 min. The results were analyzed by IMARIS 8.0 software and plotted (*C*). Statistical analyses were performed using Student's paired *t* tests ($n = 4$ per group). *Scale bars*, 100 μm. Data are presented as mean ± S.E. (*error bars*). *, $p < 0.05$. *N/S*, not significant; *Con*, control.

tion was stimulated with MCP-1 added to the lower chamber. One group of monocytes was pretreated with P5 peptide 20 min before the experiment. Transmigration was evaluated after 3 h by confocal microscopy and analyzed by IMARIS software (Fig. 7*B*). We did not detect an effect of P5 on transmigration that corresponds to the relatively low level of integrin $\alpha_D\beta_2$ on the circulatory monocytes (Fig. 7*C*).

To test a contribution of P5 peptide to macrophage migration in the matrix, we used an *in vitro* 3D migration assay in fibrin gel (Fig. 8*A*). Thioglycollate-induced peritoneal macrophages were isolated from WT and $\alpha_D^{-/-}$ mice and labeled with green (PKH67) or red (PKH26) fluorescent dyes, respectively. An equal number of cells was loaded on one side of a 3D fibrin gel, and MCP-1 was added to the opposite side to stimulate the migration. One group of samples was pretreated with P5 peptide. P5 was also added to the fibrin matrix. Migration was evaluated after 48 h by confocal microscopy (Fig. 8, *B* and *C*). Preincubation with P5 peptide markedly reduced migration of nonpolarized macrophages. Therefore, this experiment confirmed that P5 peptide affects migration of macrophages through ECM during acute peritoneal inflammation.

Usually, further development of inflammation promotes polarization of macrophages to the proinflammatory M1 phenotype. We recently showed that expression of $\alpha_D\beta_2$ is up-regulated on M1-polarized macrophages and $\alpha_D\beta_2$'s high expression generates a strong adhesion followed by macrophage retention (11, 12). Therefore, we hypothesized that P5 peptide treatment may have the opposite effect on the migration of M1-activated macrophages. WT and $\alpha_D^{-/-}$ peritoneal macrophages were stimulated with interferon-γ (IFNγ) for 4 days and tested in a 3D migration assay in the fibrin matrix. As we have shown previously, M1-polarized WT macrophages demonstrate significantly lower migration compared with nonactivated macrophages; however, $\alpha_D^{-/-}$ M1 macrophages demon-

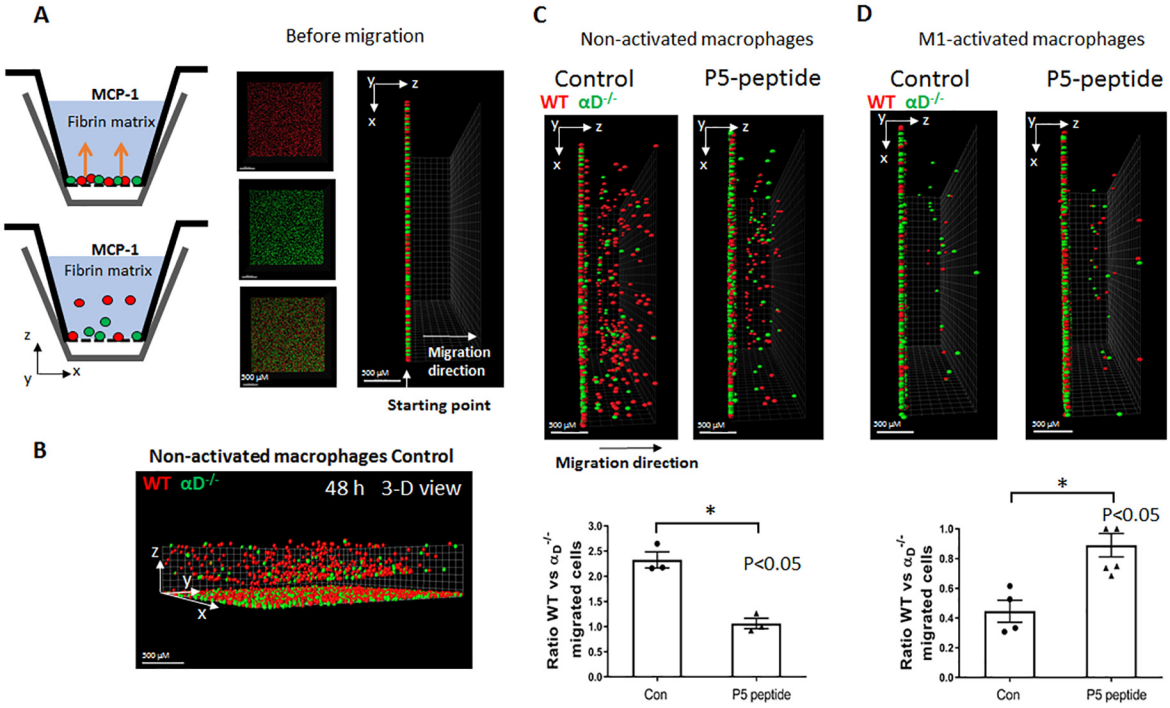

Figure 8. 3D migration of macrophages was regulated by P5 peptide. *A*, schematic representation of the experiment. Labeled cells were mixed in equal amounts and added to the Transwell. Before the initiation of migration, the background was verified by scanning samples with a confocal microscope. The migration was stimulated by adding 30 nM MCP-1 to the opposite side of the fibrin gel. *B*, after 48 h, the migration was evaluated using a Leica confocal microscope. A 3D view of the migrating cells in fibrin matrix is shown. *C* and *D*, side view of the migration of nonactivated (*C*) and M1-activated (*D*) macrophages. The results were analyzed and reconstructed by IMARIS 8.0 software. Statistical analyses were performed using Student's paired *t* tests ($n = 4$ per group). *Scale bars*, 500 μm. Data are presented as mean ± S.E. (*error bars*). *, $p < 0.05$. *Con*, control.

strate enhanced migration compared with WT (Fig. 8*D*, *left panel*). Accordingly, the addition of P5 peptide improved migratory properties of WT M1 macrophages (Fig. 8*D*, *right panel*). Apparently, P5-mediated inhibition of $\alpha_D\beta_2$ adhesion induces macrophage migration. Notably, the migration of $\alpha_D{}^{-/-}$ macrophages is not significantly changed after P5 peptide treatment, which is in agreement with our previous observations (Fig. 4*C*). Based on these results, we can predict that the effect of P5 peptide on the development of chronic inflammation would be more complex and would include inhibition of macrophage migration to the site of inflammation and inhibition of macrophage retention at the site of inflammation.

Inhibition of macrophage accumulation in the adipose tissue of diabetic mice by P5 peptide

To test P5 effects on chronic inflammation, we analyzed an accumulation of macrophages in adipose tissue of prediabetic mice. Mice after 8 weeks on a high-fat diet were injected with fluorescently labeled WT (PKH26 red) and $\alpha_D{}^{-/-}$ (PKH67 green) monocytes. One group was injected with cyclic P5 peptide; another group was injected with the control. After 48 h, the number of red- and green-labeled macrophages in the adipose tissue was evaluated using classical FACS (Fig. 9*A*) and imaging flow cytometry (Fig. 9*B*). We have previously shown that α_D deficiency reduced macrophage accumulation in the adipose tissue. Now, we demonstrate that P5 peptide possesses a similar effect on WT macrophages. The accumulation of P5-treated WT macrophages was reduced by 2.5-fold. Interestingly, the migration of $\alpha_D{}^{-/-}$ macrophages was not affected. Specifically, the ratio of WT to $\alpha_D{}^{-/-}$ macrophages in adipose tissue of control mice was 3-fold, whereas this ratio was reduced to 1 after P5 peptide treatment (Fig. 9, *C* and *D*).

Discussion

Our previous results demonstrated that modification of ECM proteins with the product of DHA oxidation, CEP, generates new inflammation-specific substrates in the tissue (19). We found that CEP is a ligand for $\alpha_D\beta_2$- and $\alpha_M\beta_2$-mediated macrophage adhesion and migration (19). Importantly, we and others detected CEP-modified proteins in different inflamed tissues such as atherosclerotic lesions, pathological angiogenesis, adipose tissue during diabetes, and peritoneal tissue during sterile inflammation (19, 22, 30, 31). Our other recent results demonstrated that the up-regulation of integrin $\alpha_D\beta_2$ at the site of inflammation promotes strong adhesion of macrophages to the substrate, related macrophage retention, and disease progression (11).

The proposed study was designed to develop an inhibitor of $\alpha_D\beta_2$-medited adhesion of macrophages to the inflamed ECM, focusing on CEP as an inflammation-specific ligand. Because $\alpha_M\beta_2$ and $\alpha_D\beta_2$ have different, rather opposite roles during chronic inflammation (11, 12, 16, 18), our goal was to identify an inhibitor that will work specifically only with integrin $\alpha_D\beta_2$. The lack of commercially available monoclonal antibodies against $\alpha_D\beta_2$ as well as a focus on specific $\alpha_D\beta_2$ ligand led us to search for a peptide-based inhibitor. Based on different affinities between CEP–α_D I-domain (K_D, 1.81×10^{-7}) and CEP–α_M I-domain (K_D, 2.1×10^{-6}) (19), we hypothesized that ligand-

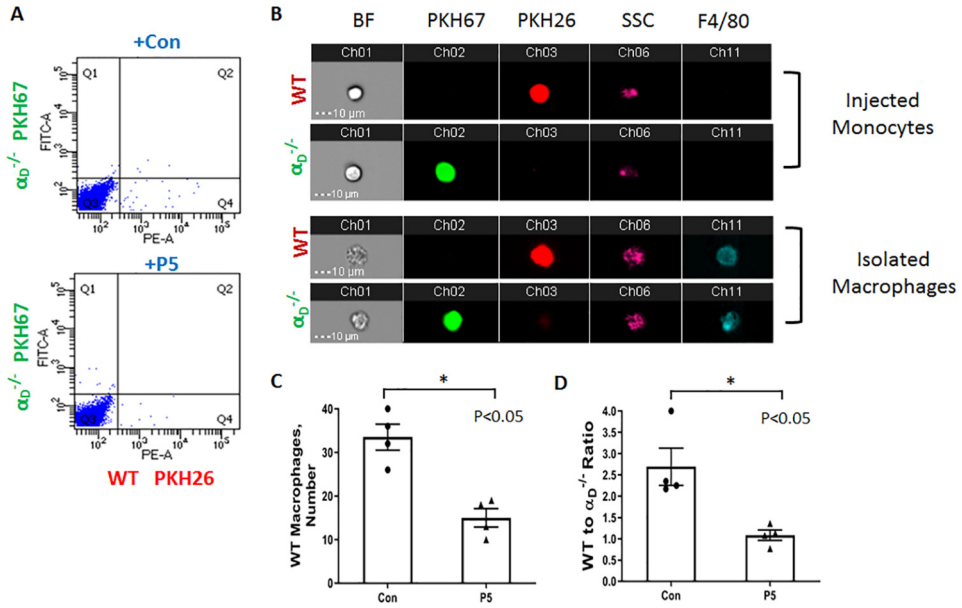

Figure 9. P5 peptide inhibited accumulation of macrophages in adipose tissue of mice during diet-induced diabetes. Isolated WT and $\alpha_D^{-/-}$ bone marrow monocytes were labeled with red PKH26 (WT) or green PKH67 ($\alpha_D^{-/-}$) fluorescent dyes, respectively; mixed in an equal amount; and injected into the tail veins of WT mice fed a high-fat diet (45% kcal from fat) for 8 weeks. Experimental groups were intraperitoneally injected with 100 μg/mouse P5 (63.45 μM) peptide 20 min before the injection of labeled cells. After 3 days, visceral adipose tissue was isolated, digested, and analyzed using flow cytometry. *A*, *Q1* and *Q4* quadrants represent the labeled cells in digested adipose tissue. *B*, imaging flow cytometry. The *upper panels* represent the injected monocytes, isolated from WT and $\alpha_D^{-/-}$ mice, labeled with red and green fluorescent dyes, respectively. The *lower panels* represent macrophages isolated from adipose tissue. The population of single, alive cells was analyzed on red and green channels. Channel 1 (*Ch01*), brightfield (*BF*), channel 2 (*Ch02*), 488-nm wavelength (PKH67); channel 3 (*Ch03*), 566-nm wavelength (PKH26); channel 6 (*Ch06*), side scattering (*SSC*); channel 11 (*Ch11*), F4/80 represents macrophage staining. *C*, macrophage number was calculated based on flow cytometry data and presented as mean ± S.E. (*error bars*). *, $p < 0.05$. *D*, the ratio of WT and $\alpha_D^{-/-}$ macrophages in each mouse was calculated and presented as mean ± S.E. (*error bars*). *, $p < 0.05$. *Con*, control; *PE*, phycoerythrin.

binding sites for CEP within $\alpha_D\beta_2$ and $\alpha_M\beta_2$ have a different structure.

We selected the γ-module of fibrinogen for the generation of a cellulose-bound peptide library based on our earlier finding that the γ-module contains several independent sites that can be recognized by integrin $\alpha_M\beta_2$ (25). We also showed that $\alpha_D\beta_2$ interacts with fibrinogen via the γ-module (13). Utilizing this library, we identified three unique peptides that are specific only for binding to integrin $\alpha_D\beta_2$ (Fig. 1). The inhibitory abilities of the identified sequences were tested in a protein binding assay (surface plasmon resonance) and an adhesion assay, which narrowed our search to one peptide, called P5 (Fig. 2). P5 peptide has a strong negative charge due to six aspartic acids. Because the critical molecular group of CEP is a carboxyl group (21), P5 peptide mimics the multiple CEP modifications on a protein surface. We cannot exclude that some other peptides with strong negative charge may have a similar effect on $\alpha_D\beta_2$-mediated macrophage adhesion. However, a number of tested peptides with several aspartic/glutamic acids in the structure do not interact with α_D I-domain (Fig. S1 and Fig. 1, spots 47, 48, 58, and 59).

$\alpha_D\beta_2$ is a multiligand receptor. The previous data demonstrated that binding sites within α_D for different ligands are overlapping (13). Accordingly, we found that P5 peptide can also block the binding to vitronectin and fibrinogen, which broadens the inhibitory ability of P5. However, the K_D of α_D binding to CEP surpasses the binding to Fg or vitronectin (13, 19); therefore, during inflammation, CEP-modified proteins will be preferential ligands for $\alpha_D\beta_2$. Moreover, the formation of adducts between CEP and natural ligands of $\alpha_D\beta_2$ will promote $\alpha_D\beta_2$ interaction with these ligands via the CEP-binding site.

Integrin ligand binding requires interaction of a negatively charged amino acid of the ligand with the metal ion–dependent adhesion site (MIDAS) in the integrin I-domain structure (32). MIDAS is a binding site for Mg^{2+}, which is coordinated by five side chains of amino acids from I-domain and an acidic residue from the ligand. Such coordination stabilizes the active conformation of I-domain and promotes ligand binding (33). The ability of P5 peptide to interact with α_D I-domain in the presence of EDTA demonstrates that P5 is not involved in the interaction with MIDAS via one aspartic acid. Moreover, the lack of P5 peptide interaction with integrin α_M (Figs. 1 and 3), which contains the same MIDAS structure, confirms that the P5-binding site is located in a separate part of the I-domain. One of the potential explanations of the P5 mechanism is prevention of $\alpha_D\beta_2$ full activation. Preincubation of $\alpha_D\beta_2$ cells with P5 peptide inhibits the following activation/conformational change of $\alpha_D\beta_2$ (Fig. 3*C*), which was detected with a conformation-dependent antibody, mAb24. The binding of mAb24 reflects a conformational change from the intermediate to full activation stage. It can be mediated either by initial ligand docking or by inside-out strong signaling. It has been shown that integrin can interact with ligands with intermediate affinity (34). The ligand docking can change the integrin conformation to an active form and increase affinity of binding. Therefore, the effect of P5 peptide on $\alpha_D\beta_2$ binding to different ligands can be explained by prevention of the conformational change from the intermediate to the active stage. Further studies are required to localize the binding motif for P5 peptide within $\alpha_D\beta_2$.

Mouse and human integrins α_D have a high level of homology (identity, 71%). CEP formation is similar in human and mouse tissues (35). P5 peptide inhibited the binding of CEP to human α_D I-domain, human $\alpha_D\beta_2$–transfected HEK 293 cells, and mouse macrophages *in vitro* and *in vivo*. Therefore, P5 peptide represents the common inhibitor for human and mouse systems.

To evaluate the effect of P5 peptide *in vivo*, a mouse peritoneal model of inflammation was applied. Thioglycollate-induced peritoneal inflammation represents a sterile acute inflammation. In contrast to chronic inflammatory diseases, the expression of integrin $\alpha_D\beta_2$ on peritoneal macrophages is intermediate (10). However, this model is commonly used to study the mechanism of neutrophil and macrophage migration and provided important information regarding the effect of P5 peptide inhibition *in vivo*. Macrophage accumulation in the peritoneal cavity at 72 h after injection of sterile thioglycollate allows tracking monocyte recruitment and macrophage efflux during inflammation (36–38). We demonstrated the specificity of P5 peptide–mediated inhibition because P5 peptide significantly blocked accumulation of WT and $\alpha_M^{-/-}$ macrophages but had no effect on the accumulation of α_D-deficient macrophages in the peritoneal cavity (Fig. 4).

The monocyte/macrophage recruitment to and efflux from the peritoneal cavity is a complex process that can be divided into several stages: translocation of monocytes from bone marrow/spleen, monocyte transmigration through the endothelium, migration via ECM, and efflux from the cavity to lymphatics. Because each step is regulated by leukocyte integrins, we tested a potential role of P5 in these processes. Using adoptively transferred macrophages, we found that P5 peptide has no effect on macrophage efflux from the peritoneal cavity (Fig. 6). This corresponds to the previous results that macrophage efflux is regulated by integrin $\alpha_4\beta_1$ (37, 38) and $\alpha_M\beta_2$ (36). In contrast, the injection of fluorescently labeled monocytes to the bloodstream in the presence of P5 peptide significantly reduced the accumulation of labeled macrophages in the peritoneal cavity (Fig. 5). This result demonstrated that P5 peptide inhibits monocyte endothelial transmigration and/or migration via ECM (peritoneal wall) toward the cavity. Also, this result indicated that the P5 effect is not related to monocyte translocation from the bone marrow. These data are in agreement with the fact that $\alpha_D\beta_2$ has a low expression on monocyte progenitors that reduces the potential contribution of $\alpha_D\beta_2$ to this step (39).

To further determine the role of P5 peptide in the recruitment, we tested P5 in monocyte transmigration (Fig. 7) and migration through the extracellular matrix *in vitro* (Fig. 8). We did not detect a difference in monocyte transmigration via the endothelial monolayer in the presence of P5 peptide. This corresponds to the previous results that monocyte diapedesis depends on integrins $\alpha_L\beta_2$, $\alpha_4\beta_1$, and to some extent $\alpha_M\beta_2$ (40–42). It also in agreement with our previous data that α_D deficiency does not change transmigration of monocytes during atherogenesis (11).

In contrast to these data, P5 had a strong effect on the migration of WT macrophages in a 3D matrix. Macrophages can apply a mesenchymal (adhesion-dependent) or amoeboid (adhesion-independent) migration mode in the 3D environment (43–47). We recently found that integrin $\alpha_D\beta_2$ can regulate mesenchymal migration (12), and the density of $\alpha_D\beta_2$ on macrophage surfaces is important for this outcome. The interplay between integrin density and cell migration is based on the theory of cell migration, which postulates that intermediate adhesion supports migration, whereas very strong adhesion will inhibit cell locomotion (48, 49). In our current experiments, we used nonactivated peritoneal macrophages, which have a moderate level of $\alpha_D\beta_2$ expression (10). Clearly, α_D deficiency reduced migration of nonactivated macrophages (Fig. 8*C*, *left panel* ($\alpha_D^{-/-}$ *green* fluorescence *versus* WT *red* fluorescence)), which confirmed a supportive role of $\alpha_D\beta_2$ in migration. Accordingly, P5 peptide reduced the migration of WT nonactivated macrophages (Fig. 8*C*, *right panel*) but did not have an effect on migration of α_D-deficient macrophages.

In our previous project, we found that high expression of $\alpha_D\beta_2$ on M1 macrophages serves to inhibit cell migration due to strong adhesion (11, 12). We verified this result by demonstrating a reduced migration of α_D-deficient M1-activated macrophages (*green* fluorescence) (Fig. 8*D*, *left panel*). Accordingly, the migration of WT M1-activated macrophages in the presence of P5 peptide was improved because $\alpha_D\beta_2$-mediated adhesion was reduced (Fig. 8*D*, *right panel*). The migration of α_D-deficient macrophages (*green* fluorescence) surpassed WT (*red* fluorescence) in the control sample but had a similar level after P5 treatment (Fig. 8, *C* and *D*). These data demonstrate that P5 peptide may differently affect macrophage migration depending on the subset of macrophages and level of $\alpha_D\beta_2$ expression on the surface. The obtained result is in agreement with our previous data that integrin $\alpha_D\beta_2$ has a different role during migration depending on receptor density on the cell surface (10, 12). The intermediate expression of $\alpha_D\beta_2$ during acute inflammation supports macrophage migration to the site of inflammation (50), whereas up-regulation of $\alpha_D\beta_2$ on proinflammatory macrophages promotes macrophage retention at the site of chronic inflammation.

To further confirm that P5 may affect macrophage accumulation during chronic inflammation, we applied the model of diet-induced insulin resistance. Recently, we demonstrated that α_D deficiency improved glucose tolerance and reduced insulin resistance in C57BL6 mice (12). Using adoptive transfer of fluorescently labeled WT and $\alpha_D^{-/-}$ monocytes, we demonstrated that the ratio of WT to $\alpha_D^{-/-}$ macrophages in the adipose tissue was reduced after P5 peptide treatment (Fig. 9). Macrophage accumulation in adipose tissue is a critical marker of inflammation and development of diabetes. This result confirmed the important role of integrin $\alpha_D\beta_2$ in the development of inflammation and proposes P5 peptide as a potential tool for the development of an anti-inflammatory treatment that can prevent macrophage accumulation and the development of different inflammatory diseases, particularly type 2 diabetes.

Materials and methods

Reagents

Reagents were purchased from Sigma-Aldrich and Thermo Fisher Scientific (Waltham, MA). Human fibrinogen and thrombin were obtained from Enzyme Research Laboratories

(South Bend, IN). The synthesis of peptides (P-con, WNGRT-STADYAMFKV; P3, AGHLNGVYYQGGTYSKAS; P4, TGT-TEFWLGNEKIHL; P5, GDAFDGFDFGDDPSD; and cyclic P5) was carried out by Peptide 2.0 Inc. (Chantilly, VA). The cyclization was done by amide cyclization from N to C terminus. The schematic sequence of cyclic peptide is shown in Fig. S1. Recombinant mouse IFNγ was purchased from Thermo Fisher Scientific. Phorbol 12-myristate 13-acetate was purchased from Sigma. Recombinant murine JE/MCP-1 (CCL2) was purchased from PeproTech (Rocky Hill, NJ). Anti-human α_D mAb (clone 240I) was generously provided by Eli Lilly Corp. Mouse FITC- and allophycocyanin-conjugated anti-α_M mAb (clone M1/70) and F4/80 mAbs were from eBioscience (San Diego, CA). The conformation-dependent antibody mAb24 against β_2 integrin was from Hycult Biotechnology (The Netherlands). mAb44a directed against the human α_M integrin subunit was purified from the conditioned media of the hybridoma cell line obtained from American Type Culture Collection (ATCC, Manassas, VA) using protein A-agarose (GE Healthcare). PKH26 (red) and PKH67 (green) fluorescent dyes were purchased from Sigma.

Animals

WT (C57BL/6J), integrin α_D-deficient (B6.129S7-*Itgad*^{tm1Bll}/J), and integrin α_M-deficient (B6.129S4-*Itgam*^{tm1Myd}/J) mice were bought from The Jackson Laboratory (Bar Harbor, ME). α_D-deficient and α_M-deficient mice were backcrossed to C57BL/6 for at least 10 generations. To develop insulin-resistant mice, C57BL/6 WT mice were fed a high-fat diet with 45% kcal from fat (TD08811, Envigo) for 8 weeks. All procedures were performed according to animal protocols approved by the East Tennessee State University Institutional Animal Care and Use Committee.

Expression and isolation of recombinant α_D and α_M I-domains in active and nonactive conformations

The constructs for α_D I-domains and α_M I-domains were generated, and recombinant proteins were isolated as described in our previous studies (13, 19). Briefly, α_D in the nonactive conformation (Pro^{128}–Ala^{323}) and α_M in the active conformation (Glu^{123}–Lys^{315}) were inserted into PGEX4T-1 vector. In "active" α_M I-domains, the unpaired Cys^{128} was substituted to Ser to prevent I-domain dimerization. Proteins were expressed in *Escherichia coli* and purified using affinity chromatography on GSH-agarose, and its fusion part was removed by thrombin. α_D in the active conformation (Pro^{128}–Lys^{314}) was inserted in pET15b vector, expressed in *E. coli* as a His tag fusion protein, and purified using affinity chromatography on Ni-chelating agarose (Qiagen Inc., Valencia, CA).

Analyses of the α_D I-domain binding to CEP, Fg, and P5 peptide by surface plasmon resonance and biolayer interferometry

The interaction between I-domains and CEP or fibrinogen in the presence of P3, P4, and P5 peptides was measured using surface plasmon resonance (Biacore 3000 instrument, Biacore, Uppsala, Sweden) as we described previously (13, 22). Fibrinogen and CEP conjugated to albumin were immobilized on the CM5 biosensor chip using standard amine coupling chemistry (1000 response units/flow cell). Steady-state experiments were performed at room temperature in 10 mM HEPES (pH 7.4) buffer containing 150 mM NaCl, 1 mM $MgCl_2$, 1 mM $CaCl_2$, and 0.005% surfactant P20 at a flow rate of 20 μl/min. Surface plasmon resonance sensorgrams were obtained by injecting various concentrations of α_D and α_M I-domains. In some samples, analytes were preincubated with blocking peptides for 15 min at room temperature. All data were corrected for the response obtained using a blank reference flow cell that was activated with *N*-ethyl-*N*′-(dimethylaminopropyl)carbodiimide/*N*-hydroxysuccinimide and then blocked with ethanolamine. Nonspecific binding to the blank flow cell was subtracted. The chip surfaces were regenerated by injecting a short pulse of 25 mM NaOH. The resulting sensorgrams were analyzed in overlay plots using BIAevaluation software (version 4.01, GE Healthcare).

The interaction between the α_D I-domain (in active and nonactive conformations) and P5 peptide was measured using biolayer interferometry (ForteBio, Fremont, CA). N-terminally biotinylated P5 peptide was immobilized on a streptavidin biosensor. Different concentrations of the I-domains in 20 mM HEPES (pH 7.4) buffer containing 150 mM NaCl, 1 mM $MgCl_2$, 1 mM $CaCl_2$, and 0.05% Tween 20 were added to immobilized P5 peptide. For some experiments, Mg^{2+} and Ca^{2+} were exchanged for 5 mM EDTA. All data were corrected for the response obtained using a blank reference biosensor. The biosensor surface was regenerated using 2 M NaCl and 25 mM NaOH. Data were analyzed using the ForteBio Data Analysis 11.0 program (ForteBio).

Synthesis of cellulose-bound peptide library

The fibrinogen γ-module–derived peptide library assembled on a single cellulose membrane support was prepared by parallel spot synthesis as described previously (25, 26). The libraries were synthesized as 9-mer overlapping peptides with a 3-amino-acid offset. Peptides were C-terminally attached to the cellulose via a (β-Ala)$_2$ spacer and were acetylated N-terminally. The membrane-bound peptides were tested for their ability to bind the α_M I-domain and α_D I-domain. In brief, membranes were blocked with 1% BSA and incubated with 5 μg/ml ^{125}I-labeled α_M I-domain or α_D I-domain in 20 mM Tris buffer solution containing 1 mM $MgCl_2$, 0.1% BSA, and 2 mM DTT. Membranes were washed with Tris buffer solution containing 0.05% Tween 20 and dried, and α_M and α_D I-domain binding was visualized by autoradiography and analyzed by densitometry.

Flow cytometry analysis

Flow cytometry analysis was performed to assess the expression and activation of receptors on the surface of cells transfected with $\alpha_D\beta_2$, $\alpha_M\beta_2$, and $\alpha_L\beta_2$ integrins and to evaluate the number of fluorescently labeled mouse macrophages isolated from the peritoneal cavity or adipose tissue. Transfected HEK 293 cells were incubated with anti-α_D (clone 240I), anti-α_M (clone M1/70), and anti-β_2 (clone IB4) antibodies and analyzed using Fortessa X-20 (BD Biosciences) as described (13, 24). The isolated prelabeled WT (red PKH26) bone marrow–derived macrophages, peritoneal macrophages, or adipose tissue macrophages (WT, red; $\alpha_D^{-/-}$, green) were washed with PBS,

counted, and analyzed by flow cytometry (Fortessa X-20) and imaging flow cytometry (ImageStream Mark II, Amnis). Macrophage numbers were calculated based on the percentage of F4/80-positive population in flow cytometry.

Cell adhesion assay

The adhesion assay was performed as described previously with modifications (13, 24). Briefly, 96-well plates (Immulon 2HB, Cambridge, MA) were coated with fibrinogen, CEP, P5, or vitronectin for 3 h at 37 °C. The wells were postcoated with 0.5% polyvinyl alcohol for 1 h at 37 °C. HEK 293 cells transfected with $\alpha_M\beta_2$, $\alpha_X\beta_2$, or $\alpha_D\beta_2$ integrins were labeled with 10 μM Calcein AM (Molecular Probes, Eugene, OR) for 20 min at 37 °C, washed with Dulbecco's modified Eagle's medium, and resuspended in the same medium at a concentration of 1×10^6 cells/ml. Aliquots (50 μl) of the labeled cells were added to each well. For inhibition experiments, cells were mixed with various concentration of peptides (P3, P4, and P5) and incubated for 20 min at 37 °C before they were added to the ligand-coated wells. After 30 min of adhesion at 37 °C in a 5% CO_2 humidified atmosphere, the nonadherent cells were removed by washing with Hanks' balanced salt solution. The fluorescence was measured in a Synergy H1 fluorescence plate reader (BioTek, Winooski, VT), and the number of adherent cells was determined from a labeled control.

Isolation of peritoneal macrophages and activation of M1 macrophages

WT and $\alpha_D{}^{-/-}$ 8–10-week-old mice were intraperitoneally injected with 1 ml of 4% thioglycollate, and 3 days later, peritoneal cells were harvested with 5 ml of sterile PBS by lavage of the peritoneal cavity. The cells were washed with PBS and resuspended in RPMI 1640 medium. The cell suspension was transferred into 100-mm Petri dishes and incubated for 2 h at 37 °C in humidified air containing 5% CO_2 atmosphere. Nonadherent cells were washed out with RPMI 1640 medium, and the adherent macrophages were replenished with RPMI 1640 medium. The macrophages were differentiated to M1 phenotype by treatment with recombinant mouse IFNγ (100 units/ml) for 4 days. Medium with IFNγ was changed every 2 days or as required. The M1-phenotype macrophages from WT and $\alpha_D{}^{-/-}$ mice were labeled with red fluorescent marker PKH26 and green fluorescent marker PKH67, respectively, according to the manufacturer's instructions (Sigma-Aldrich). The fluorescently labeled cells were dissociated from the plates using 5 mM EDTA in PBS and used for the experiments thereafter.

Adoptive transfer in the recruitment of macrophages to the peritoneal cavity

The approach is based on our previous publication with some modifications (11). Bone-marrow monocytes were isolated from WT mice using a magnetic bead separation kit (Miltenyi Biotec, Gaithersburg, MD). Monocytes were labeled with red PKH26 (WT) fluorescent dye. Recipient WT mice were intraperitoneally injected with 100 μg/mouse P5 (63.4 μM) peptide. After 20 min, 1 ml of 4% thioglycollate was intraperitoneally injected to all mice to induce inflammation. Then fluorescently labeled WT (red PKH26 dye) bone marrow monocytes were injected into the tail veins of the recipient mice. After 72 h, the peritoneal macrophages were harvested and assessed by fluorescence microscopy and flow cytometry (Fortessa X-20).

Adoptive transfer in macrophage efflux from the peritoneal cavity

The adoptive transfer was performed as described previously with some modifications (11). Briefly, recipient and donor WT mice were intraperitoneally injected with 4% thioglycollate. After 48 h, macrophages were isolated from the peritoneal cavity of donor mice, labeled with PKH26 red fluorescent dye, and injected into the peritoneal cavity of the recipient mice (1×10^6 cells/mouse). Immediately, the recipient mice were intraperitoneally injected with 100 μg/mouse P5 (63.4 μM) peptide or control. After an additional 24 h, macrophages were harvested from the peritoneal cavity and counted, and the number of fluorescently labeled macrophages was assessed by fluorescence microscopy and flow cytometry (Fortessa X-20).

Adoptive transfer in the model of diet-induced diabetes

The adoptive transfer was performed as described previously (12). Briefly, WT and $\alpha_D{}^{-/-}$ bone marrow monocytes were isolated and purified by a magnetic bead separation kit (Miltenyi Biotec); labeled with red PKH26 (WT) or green PKH67 ($\alpha_D{}^{-/-}$) fluorescent dye, respectively; mixed in an equal amount (1×10^6 cells/color/mouse); and injected into the tail veins of WT mice fed a high-fat diet (45% kcal from fat) for 8 weeks. Mice in the experimental group were intraperitoneally injected with 100 μg/mouse P5 (63.4 μM) peptide 20 min before the injection of labeled cells. After 3 days, visceral adipose tissue was isolated, digested, and analyzed using flow cytometry (Fortessa X-20) and imaging flow cytometry (ImageStream Mark II).

Transendothelial migration assay

HUVECs were seeded at 10^5 cells/well in the upper chamber of Transwell inserts (diameter, 6.5 mm; pore size, 5.0 μm; Corning), labeled with PKH67 green fluorescence, and cultured overnight in vascular cell basal medium with vascular endothelial growth factor (ATCC). On the next day, isolated bone marrow monocytes were labeled with PKH26 red fluorescent dye and added to the top of endothelial cells, and MCP-1 was added to the lower chamber of the wells to stimulate the migration of monocytes. In some experiments, the monocytes were preincubated with 200 μg/ml P5 (126.8 μM) peptide for 20 min. After 3-h incubation at 37 °C, the number of migrated cells was determined by a Leica confocal microscope, and the results were reconstructed and analyzed using IMARIS 8.0 software.

Migration of macrophages in 3D fibrin gel

The migration assay was performed as described previously (12, 19). WT and $\alpha_D{}^{-/-}$ peritoneal nonactivated macrophages were labeled with PKH26 red fluorescent dye and PKH67 green fluorescent dye, respectively. The cell migration assay was performed for 48 h at 37 °C in 5% CO_2 in a sterile condition. An equal number of WT and $\alpha_D{}^{-/-}$ macrophages was evaluated by cytospin of mixed cells before the experiment and at the start-

ing point before migration. Labeled WT (1.5×10^5) and $\alpha_D^{-/-}$ (1.5×10^5) activated macrophages were plated on the membranes of Transwell inserts with a pore size of 8 μm and 6.5 mm in diameter (Costar, Corning) precoated with Fg. Fibrin gel (100 μl/sample) was generated by mixing 0.75 mg/ml Fg containing 1% fetal bovine serum, 1% penicillin/streptomycin, and 0.5 unit/ml thrombin. 30 nM MCP-1 was added on the top of the gel to initiate the migration. Migrating cells were detected by a Leica TCS SP8 confocal microscope, and the results were analyzed and reconstructed using IMARIS 8.0 software.

Statistical analysis

Statistical analyses were performed using Student's *t* test or Student's paired *t* tests where indicated in the text using SigmaPlot 13. A value of $p < 0.05$ was considered significant.

Author contributions—K. C. and V. P. Y. conceptualization; K. C., T. V. B., and V. P. Y. data curation; K. C., N. P. P., and V. P. Y. formal analysis; K. C., N. P. P., W. B., E. S., and V. P. Y. investigation; K. C. and E. A. P. methodology; K. C., E. A. P., T. V. B., and V. P. Y. writing-review and editing; V. P. Y. funding acquisition; V. P. Y. writing-original draft; V. P. Y. project administration.

Acknowledgment—We thank Dr. Tatiana Ugarova for the valuable advice on the experimental design and preparation of peptide library.

References

1. Alexandraki, K., Piperi, C., Kalofoutis, C., Singh, J., Alaveras, A., and Kalofoutis, A. (2006) Inflammatory process in type 2 diabetes: the role of cytokines. *Ann. N.Y. Acad. Sci.* **1084,** 89–117 CrossRef Medline
2. Ouchi, N., Kihara, S., Funahashi, T., Matsuzawa, Y., and Walsh, K. (2003) Obesity, adiponectin and vascular inflammatory disease. *Curr. Opin. Lipidol.* **14,** 561–566 CrossRef Medline
3. Subramanian, S., and Chait, A. (2009) The effect of dietary cholesterol on macrophage accumulation in adipose tissue: implications for systemic inflammation and atherosclerosis. *Curr. Opin. Lipidol* **20,** 39–44 CrossRef Medline
4. Schittenhelm, L., Hilkens, C. M., and Morrison, V. L. (2017) β2 integrins as regulators of dendritic cell, monocyte, and macrophage function. *Front. Immunol.* **8,** 1866 CrossRef Medline
5. Danilenko, D. M., Rossitto, P. V., Van der Vieren, M., Le Trong, H., McDonough, S. P., Affolter, V. K., and Moore, P. F. (1995) A novel canine leukointegrin, αdβ2, is expressed by specific macrophage subpopulations in tissue and a minor CD8+ lymphocyte subpopulation in peripheral blood. *J. Immunol.* **155,** 35–44 Medline
6. Grayson, M. H., Van der Vieren, M., Sterbinsky, S. A., Michael Gallatin, W., Hoffman, P. A., Staunton, D. E., and Bochner, B. S. (1998) αdβ2 integrin is expressed on human eosinophils and functions as an alternative ligand for vascular cell adhesion molecule 1 (VCAM-1). *J. Exp. Med.* **188,** 2187–2191 CrossRef Medline
7. Miyazaki, Y., Vieira-de-Abreu, A., Harris, E. S., Shah, A. M., Weyrich, A. S., Castro-Faria-Neto, H. C., and Zimmerman, G. A. (2014) Integrin αDβ2 (CD11d/CD18) is expressed by human circulating and tissue myeloid leukocytes and mediates inflammatory signaling. *PLoS One* **9,** e112770 CrossRef Medline
8. Thomas, A. P., Dunn, T. N., Oort, P. J., Grino, M., and Adams, S. H. (2011) Inflammatory phenotyping identifies CD11d as a gene markedly induced in white adipose tissue in obese rodents and women. *J. Nutr.* **141,** 1172–1180 CrossRef Medline
9. Van der Vieren, M., Le Trong, H., Wood, C. L., Moore, P. F., St John, T., Staunton, D. E., and Gallatin, W. M. (1995) A novel leukointegrin, $\alpha_d\beta_2$, binds preferentially to ICAM-3. *Immunity* **3,** 683–690 CrossRef Medline
10. Yakubenko, V. P., Belevych, N., Mishchuk, D., Schurin, A., Lam, S. C., and Ugarova, T. P. (2008) The role of integrin αDβ2 (CD11d/CD18) in monocyte/macrophage migration. *Exp. Cell Res.* **314,** 2569–2578 CrossRef Medline
11. Aziz, M. H., Cui, K., Das, M., Brown, K. E., Ardell, C. L., Febbraio, M., Pluskota, E., Han, J., Wu, H., Ballantyne, C. M., Smith, J. D., Cathcart, M. K., and Yakubenko, V. P. (2017) The upregulation of integrin αDβ2 (CD11d/CD18) on inflammatory macrophages promotes macrophage retention in vascular lesions and development of atherosclerosis. *J. Immunol.* **198,** 4855–4867 CrossRef Medline
12. Cui, K., Ardell, C. L., Podolnikova, N. P., and Yakubenko, V. P. (2018) Distinct migratory properties of M1, M2, and resident macrophages are regulated by αDβ2 and αMβ2 integrin-mediated adhesion. *Front. Immunol.* **9,** 2650 CrossRef Medline
13. Yakubenko, V. P., Yadav, S. P., and Ugarova, T. P. (2006) Integrin αDβ2, an adhesion receptor up-regulated on macrophage foam cells, exhibits multiligand-binding properties. *Blood* **107,** 1643–1650 CrossRef Medline
14. Wang, Y., Gao, H., Shi, C., Erhardt, P. W., Pavlovsky, A., Soloviev, D. A., Bledzka, K., Ustinov, V., Zhu, L., Qin, J., Munday, A. D., Lopez, J., Plow, E., and Simon, D. I. (2017) Leukocyte integrin Mac-1 regulates thrombosis via interaction with platelet GPIbα. *Nat. Commun.* **8,** 15559 CrossRef Medline
15. Yakubenko, V. P., Bhattacharjee, A., Pluskota, E., and Cathcart, M. K. (2011) αMβ2 integrin activation prevents alternative activation of human and murine macrophages and impedes foam cell formation. *Circ. Res.* **108,** 544–554 CrossRef Medline
16. Szpak, D., Izem, L., Verbovetskiy, D., Soloviev, D. A., Yakubenko, V. P., and Pluskota, E. (2018) αMβ2 is antiatherogenic in female but not male mice. *J. Immunol.* **200,** 2426–2438 CrossRef Medline
17. Wolf, D., Anto-Michel, N., Blankenbach, H., Wiedemann, A., Buscher, K., Hohmann, J. D., Lim, B., Bäuml, M., Marki, A., Mauler, M., Duerschmied, D., Fan, Z., Winkels, H., Sidler, D., Diehl, P., *et al.* (2018) A ligand-specific blockade of the integrin Mac-1 selectively targets pathologic inflammation while maintaining protective host-defense. *Nat. Commun.* **9,** 525 CrossRef Medline
18. Wolf, D., Bukosza, N., Engel, D., Poggi, M., Jehle, F., Anto Michel, N., Chen, Y. C., Colberg, C., Hoppe, N., Dufner, B., Boon, L., Blankenbach, H., Hilgendorf, I., von Zur Muhlen, C., Reinöhl, J., *et al.* (2017) Inflammation, but not recruitment, of adipose tissue macrophages requires signalling through Mac-1 (CD11b/CD18) in diet-induced obesity (DIO). *Thromb. Haemost.* **117,** 325–338 CrossRef Medline
19. Yakubenko, V. P., Cui, K., Ardell, C. L., Brown, K. E., West, X. Z., Gao, D., Stefl, S., Salomon, R. G., Podrez, E. A., and Byzova, T. V. (2018) Oxidative modifications of extracellular matrix promote the second wave of inflammation via β2 integrins. *Blood* **132,** 78–88 CrossRef Medline
20. Wang, H., Linetsky, M., Guo, J., Choi, J., Hong, L., Chamberlain, A. S., Howell, S. J., Howes, A. M., and Salomon, R. G. (2015) 4-Hydroxy-7-oxo-5-heptenoic Acid (HOHA) lactone is a biologically active precursor for the generation of 2-(ω-carboxyethyl)pyrrole (CEP) derivatives of proteins and ethanolamine phospholipids. *Chem. Res. Toxicol.* **28,** 967–977 CrossRef Medline
21. Gu, X., Meer, S. G., Miyagi, M., Rayborn, M. E., Hollyfield, J. G., Crabb, J. W., and Salomon, R. G. (2003) Carboxyethylpyrrole protein adducts and autoantibodies, biomarkers for age-related macular degeneration. *J. Biol. Chem.* **278,** 42027–42035 CrossRef Medline
22. Kim, Y. W., Yakubenko, V. P., West, X. Z., Gugiu, G. B., Renganathan, K., Biswas, S., Gao, D., Crabb, J. W., Salomon, R. G., Podrez, E. A., and Byzova, T. V. (2015) Receptor-mediated mechanism controlling tissue levels of bioactive lipid oxidation products. *Circ. Res.* **117,** 321–332 CrossRef Medline
23. Biswas, S., Xin, L., Panigrahi, S., Zimman, A., Wang, H., Yakubenko, V. P., Byzova, T. V., Salomon, R. G., and Podrez, E. A. (2016) Novel phosphatidylethanolamine derivatives accumulate in circulation in hyperlipidemic ApoE−/− mice and activate platelets via TLR2. *Blood* **127,** 2618–2629 CrossRef Medline
24. Yakubenko, V. P., Lishko, V. K., Lam, S. C., and Ugarova, T. P. (2002) A molecular basis for integrin $\alpha_M\beta_2$ in ligand binding promiscuity. *J. Biol. Chem.* **277,** 48635–48642 CrossRef Medline
25. Lishko, V. K., Podolnikova, N. P., Yakubenko, V. P., Yakovlev, S., Medved, L., Yadav, S. P., and Ugarova, T. P. (2004) Multiple binding sites in fibrin-

ogen for integrin αMβ2 (Mac-1). *J. Biol. Chem.* **279,** 44897–44906 CrossRef Medline
26. Podolnikova, N. P., Podolnikov, A. V., Haas, T. A., Lishko, V. K., and Ugarova, T. P. (2015) Ligand recognition specificity of leukocyte integrin αMβ2 (Mac-1, CD11b/CD18) and its functional consequences. *Biochemistry* **54,** 1408–1420 CrossRef Medline
27. Yakubenko, V. P., Solovjov, D. A., Zhang, L., Yee, V. C., Plow, E. F., and Ugarova, T. P. (2001) Identification of the binding site for fibrinogen recognition peptide γ383–395 within the α_M I-domain of integrin $\alpha_M\beta_2$. *J. Biol. Chem.* **276,** 13995–14003 CrossRef Medline
28. Ustinov, V. A., and Plow, E. F. (2002) Delineation of the key amino acids involved in NIF binding to the I-domain supports a mosaic model for the capacity of integrin $\alpha_M\beta_2$ to recognize multiple ligands. *J. Biol. Chem.* **277,** 18769–18776 CrossRef Medline
29. Zhang, L., and Plow, E. F. (1999) Amino acid sequences within the α subunit of integrin $\alpha_M\beta_2$ (Mac-1) critical for specific recognition of C3bi. *Biochemistry* **38,** 8064–8071 CrossRef Medline
30. West, X. Z., Malinin, N. L., Merkulova, A. A., Tischenko, M., Kerr, B. A., Borden, E. C., Podrez, E. A., Salomon, R. G., and Byzova, T. V. (2010) Oxidative stress induces angiogenesis by activating TLR2 with novel endogenous ligands. *Nature* **467,** 972–976 CrossRef Medline
31. Panigrahi, S., Ma, Y., Hong, L., Gao, D., West, X. Z., Salomon, R. G., Byzova, T. V., and Podrez, E. A. (2013) Engagement of platelet toll-like receptor 9 by novel endogenous ligands promotes platelet hyperreactivity and thrombosis. *Circ. Res.* **112,** 103–112 CrossRef Medline
32. Li, R., Rieu, P., Griffith, D. L., Scott, D., and Arnaout, M. A. (1998) Two functional states of the CD11b A-domain: correlations with key features of two Mn^{2+}-complexed crystal structures. *J. Cell Biol.* **143,** 1523–1534 CrossRef Medline
33. Xiong, J.-P., Li, R., Essafi, M., Stehle, T., and Arnaout, M. A. (2000) An isoleucine-based allosteric switch controls affinity and shape shifting in integrin CD11b A-domain. *J. Biol. Chem.* **275,** 38762–38767 CrossRef Medline
34. Zhu, J., Zhu, J., and Springer, T. A. (2013) Complete integrin headpiece opening in eight steps. *J. Cell Biol.* **201,** 1053–1068 CrossRef Medline
35. Salomon, R. G. (2017) Carboxyethylpyrroles: from hypothesis to the discovery of biologically active natural products. *Chem. Res. Toxicol.* **30,** 105–113 CrossRef Medline
36. Cao, C., Lawrence, D. A., Strickland, D. K., and Zhang, L. (2005) A specific role of integrin Mac-1 in accelerated macrophage efflux to the lymphatics. *Blood* **106,** 3234–3241 CrossRef Medline
37. Bellingan, G. J., Caldwell, H., Howie, S. E., Dransfield, I., and Haslett, C. (1996) *In vivo* fate of the inflammatory macrophage during the resolution of inflammation: inflammatory macrophages do not die locally, but emigrate to the draining lymph nodes. *J. Immunol.* **157,** 2577–2585 Medline
38. Bellingan, G. J., Xu, P., Cooksley, H., Cauldwell, H., Shock, A., Bottoms, S., Haslett, C., Mutsaers, S. E., and Laurent, G. J. (2002) Adhesion molecule-dependent mechanisms regulate the rate of macrophage clearance during the resolution of peritoneal inflammation. *J. Exp. Med.* **196,** 1515–1521 CrossRef Medline
39. Noti, J. D. (2002) Expression of the myeloid-specific leukocyte integrin gene CD11d during macrophage foam cell differentiation and exposure to lipoproteins. *Int. J. Mol. Med.* **10,** 721–727 Medline
40. Chuluyan, H. E., and Issekutz, A. C. (1993) VLA-4 integrin can mediate CD11/CD18-independent transendothelial migration of human monocytes. *J. Clin. Investig.* **92,** 2768–2777 CrossRef Medline
41. Shang, X. Z., and Issekutz, A. C. (1998) Contribution of CD11a/CD18, CD11b/CD18, ICAM-1 (CD54) and -2 (CD102) to human monocyte migration through endothelium and connective tissue fibroblast barriers. *Eur. J. Immunol.* **28,** 1970–1979 CrossRef Medline
42. Meerschaert, J., and Furie, M. B. (1994) Monocytes use either CD11/CD18 or VLA-4 to migrate across human endothelium *in vitro*. *J. Immunol.* **152,** 1915–1926 Medline
43. Lämmermann, T., Bader, B. L., Monkley, S. J., Worbs, T., Wedlich-Söldner, R., Hirsch, K., Keller, M., Förster, R., Critchley, D. R., Fässler, R., and Sixt, M. (2008) Rapid leukocyte migration by integrin-independent flowing and squeezing. *Nature* **453,** 51–55 CrossRef Medline
44. Bouissou, A., Proag, A., Bourg, N., Pingris, K., Cabriel, C., Balor, S., Mangeat, T., Thibault, C., Vieu, C., Dupuis, G., Fort, E., Lévêque-Fort, S., Maridonneau-Parini, I., and Poincloux, R. (2017) Podosome force generation machinery: a local balance between protrusion at the core and traction at the ring. *ACS Nano* **11,** 4028–4040 CrossRef Medline
45. Cougoule, C., Van Goethem, E., Le Cabec, V., Lafouresse, F., Dupré, L., Mehraj, V., Mège, J. L., Lastrucci, C., and Maridonneau-Parini, I. (2012) Blood leukocytes and macrophages of various phenotypes have distinct abilities to form podosomes and to migrate in 3D environments. *Eur. J. Cell Biol.* **91,** 938–949 CrossRef Medline
46. Maridonneau-Parini, I. (2014) Control of macrophage 3D migration: a therapeutic challenge to limit tissue infiltration. *Immunol. Rev.* **262,** 216–231 CrossRef Medline
47. Wiesner, C., Le-Cabec, V., El Azzouzi, K., Maridonneau-Parini, I., and Linder, S. (2014) Podosomes in space: macrophage migration and matrix degradation in 2D and 3D settings. *Cell Adh. Migr.* **8,** 179–191 CrossRef Medline
48. Palecek, S. P., Loftus, J. C., Ginsberg, M. H., Lauffenburger, D. A., and Horwitz, A. F. (1997) Integrin-ligand binding properties govern cell migration speed through cell-substratum adhesiveness. *Nature* **385,** 537–540 CrossRef Medline
49. DiMilla, P. A., Stone, J. A., Quinn, J. A., Albelda, S. M., and Lauffenburger, D. A. (1993) Maximal migration of human smooth muscle cells on fibronectin and type IV collagen occurs at an intermediate attachment strength. *J. Cell Biol.* **122,** 729–737 CrossRef Medline
50. Mabon, P. J., Weaver, L. C., and Dekaban, G. A. (2000) Inhibition of monocyte/macrophage migration to a spinal cord injury site by an antibody to the integrin αD: a potential new anti-inflammatory treatment. *Exp. Neurol.* **166,** 52–64 CrossRef Medline